Tire and road wear particles in infiltration pond sediments: Occurrence, spatial distribution, size fractionation and correlation with metals

Authors:

Tiago De Oliveira[1]*, Du Phuc Tho Dang[1], Maxime Chaillou[1], Sampriti Roy[1], Nadège Caubrière[1], Martin Guillon[1], David Mabilais[1], Sophie Ricordel[1], Liliane Jean-Soro[1], Béatrice Béchet[1], Bogdan Muresan Paslaru[2], Laurence Poirier[3], Johnny Gasperi[1]

[1] Univ Gustave Eiffel, GERS-LEE, F-44344 Bouguenais, France

[2] Univ Gustave Eiffel, AME-EASE, F-44344 Bouguenais, France

[3] Nantes Université, ISOMer, F-44000 Nantes, France

*Corresponding author: T. De Oliveira, Allée des Ponts et Chaussées, F-44344 Bouguenais, France

Email address: tiago.de-oliveira@univ-eiffel.fr

Table of contents

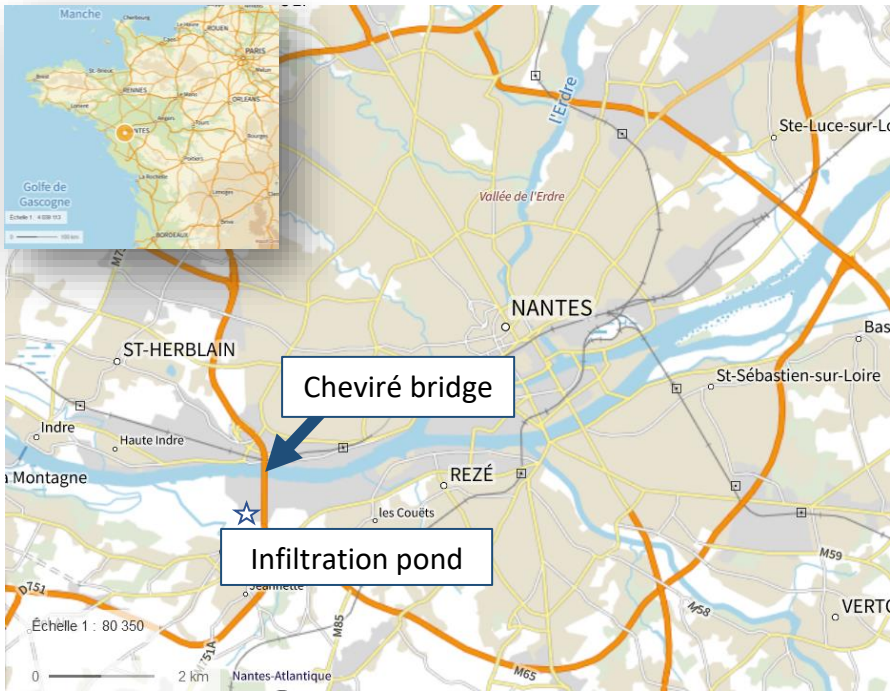

Figure SI 1: Location of the studied infiltration pond. The map was downloaded from https://www.geoportail.gouv.fr/

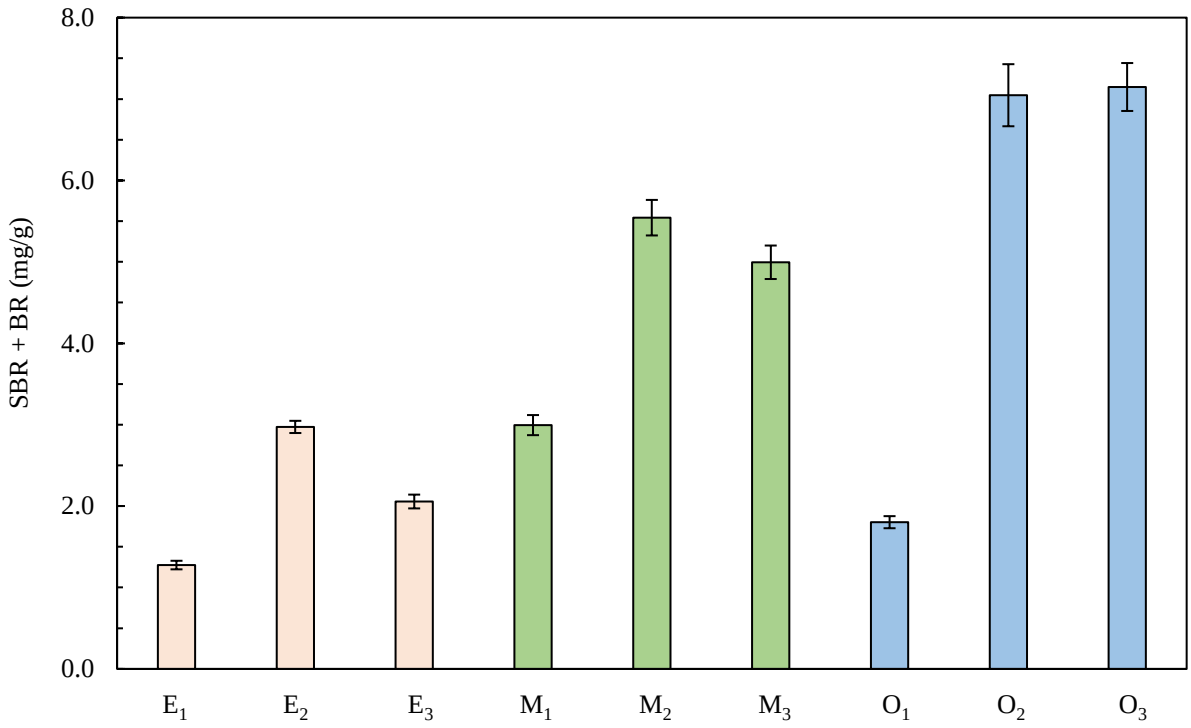

Figure SI 2: Distribution of the SBR + BR (median of replicate in mg/g) quantified in sediment sampled (< 500 µm) from the entrance (E_1, E_2, E_3 in orange), middle (M_1, M_2, M_3 in green) and overflow (O_1, O_2, O_3 in blue) sections. Error bars represent the standard deviation of the replicate (n=3).

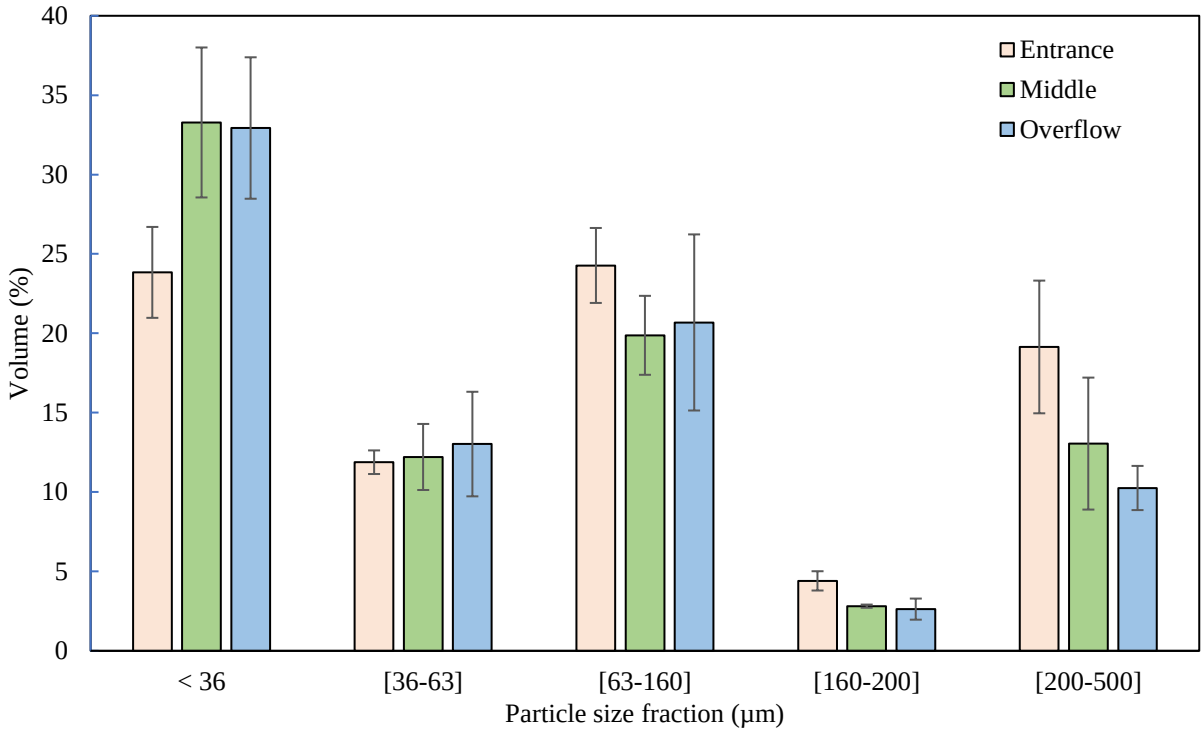

Figure SI 3: Volume proportion (%) of sediment measured with laser granulometry in five particle size fractions. A similar trend to that of the mass proportion of SBR + BR in the same five size fractions is observed, with an increase in the volume proportion of sediment towards the overflow section for particle sizes below 63 µm, and a decrease in proportion for the coarser materials (above 63 µm) towards the overflow section.

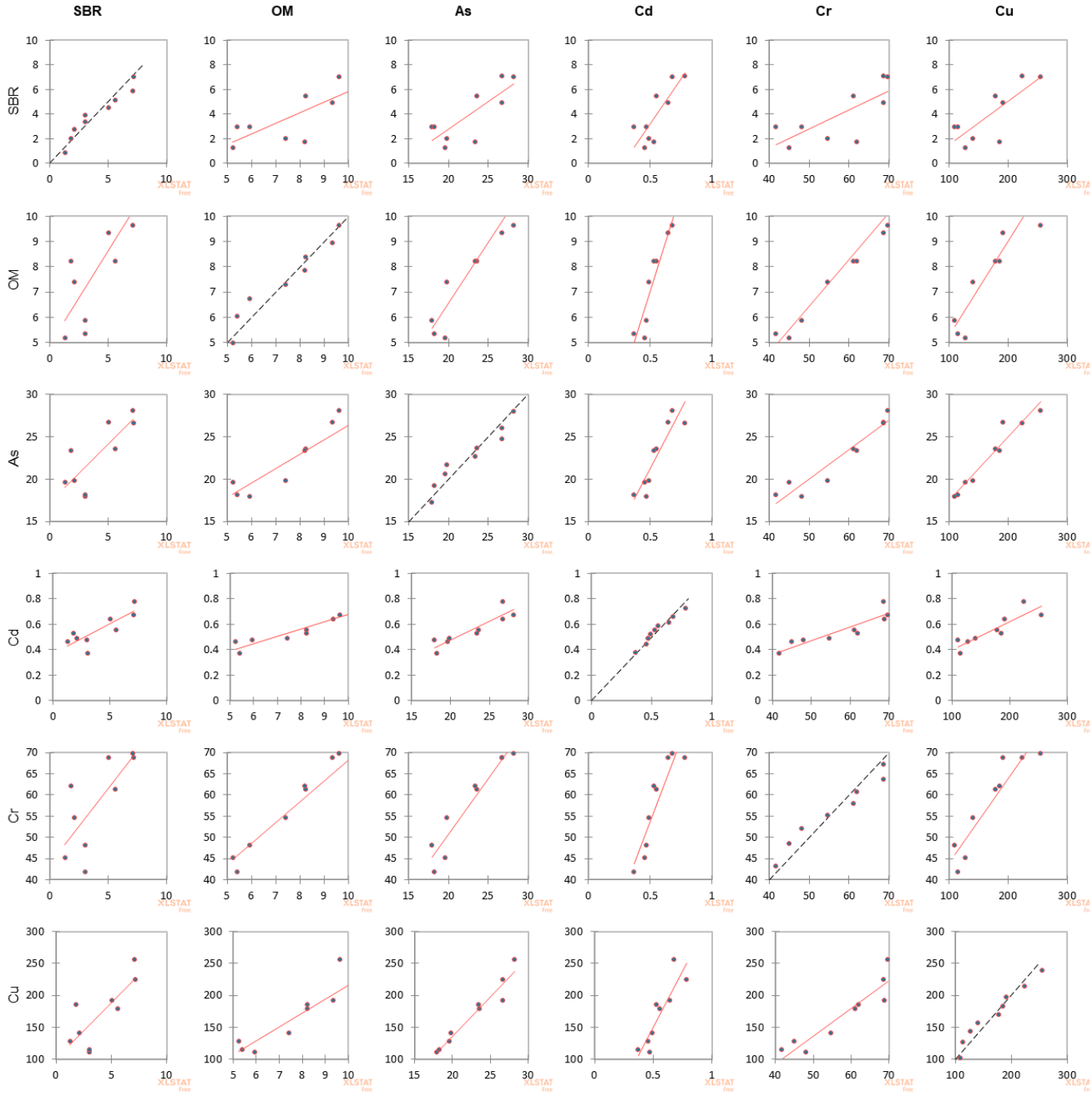

Figure SI 4a: Quantile-Quantile plots of SBR + BR, OM and metals variables using Microsoft Excel software and XLSTAT add-on.

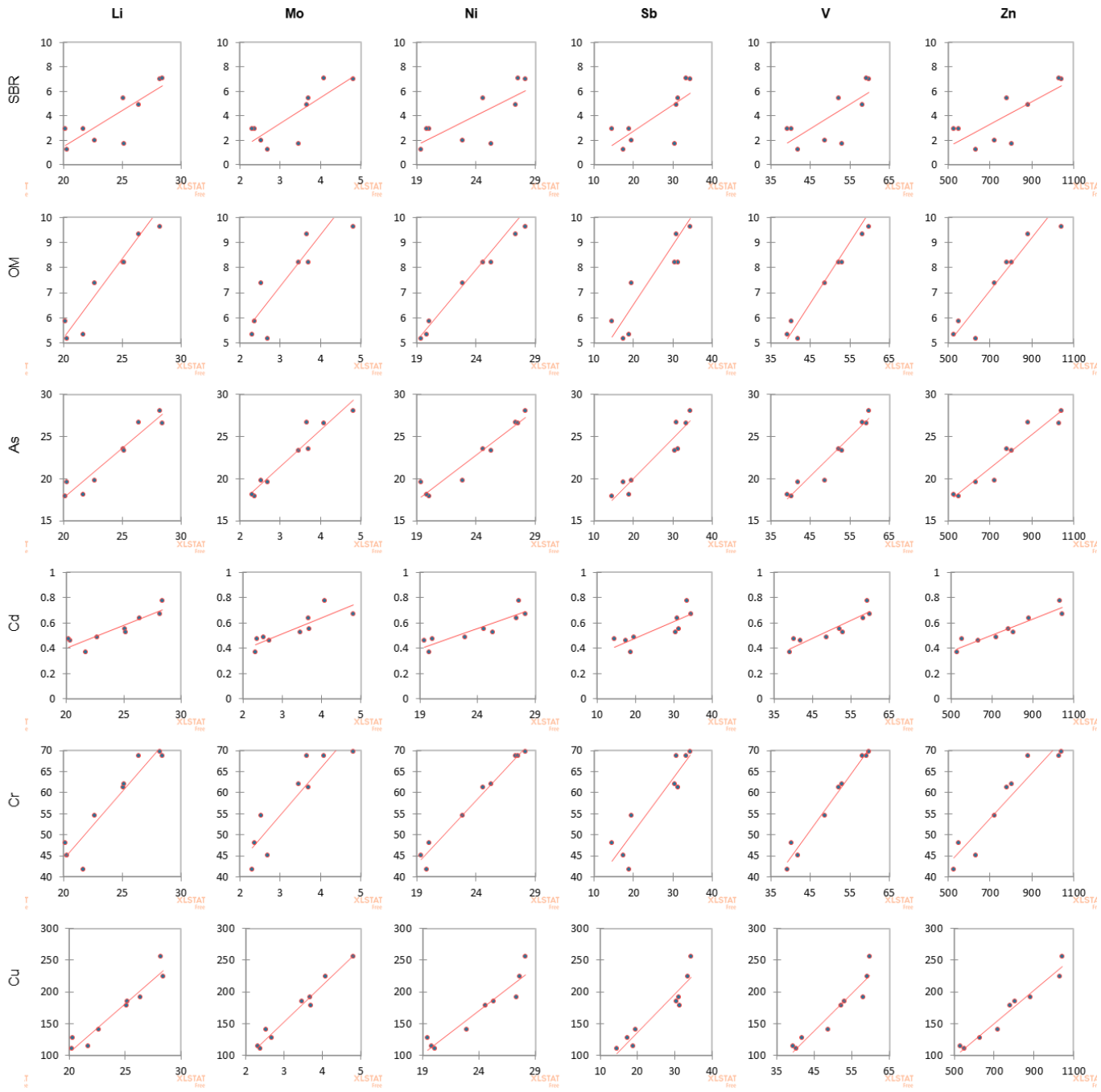

Figure SI 4b: Quantile-Quantile plots of SBR + BR, OM and metals variables using Microsoft Excel software and XLSTAT add-on.

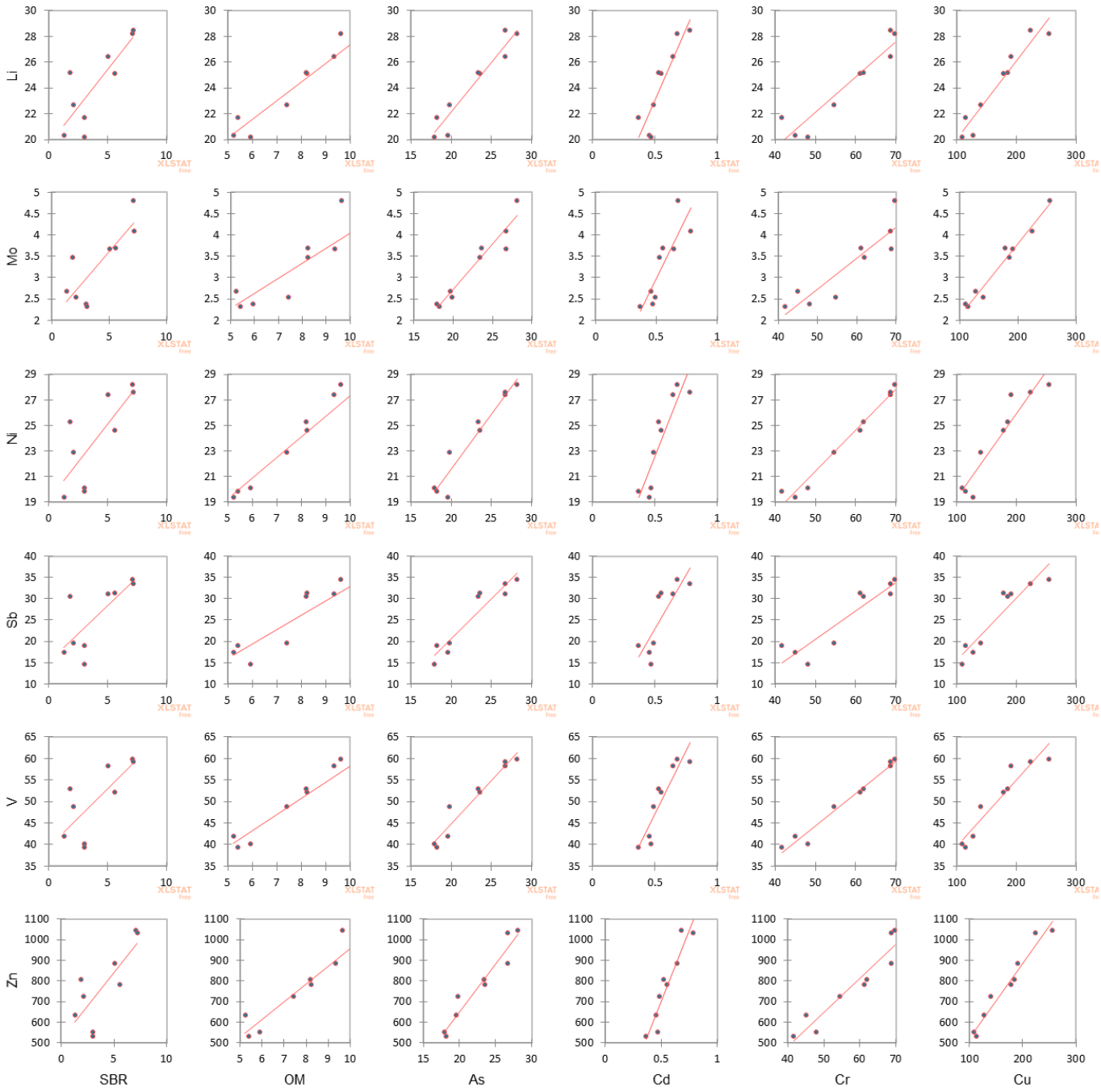

Figure SI 4c: Quantile-Quantile plots of SBR + BR, OM and metals variables using Microsoft Excel software and XLSTAT add-on.

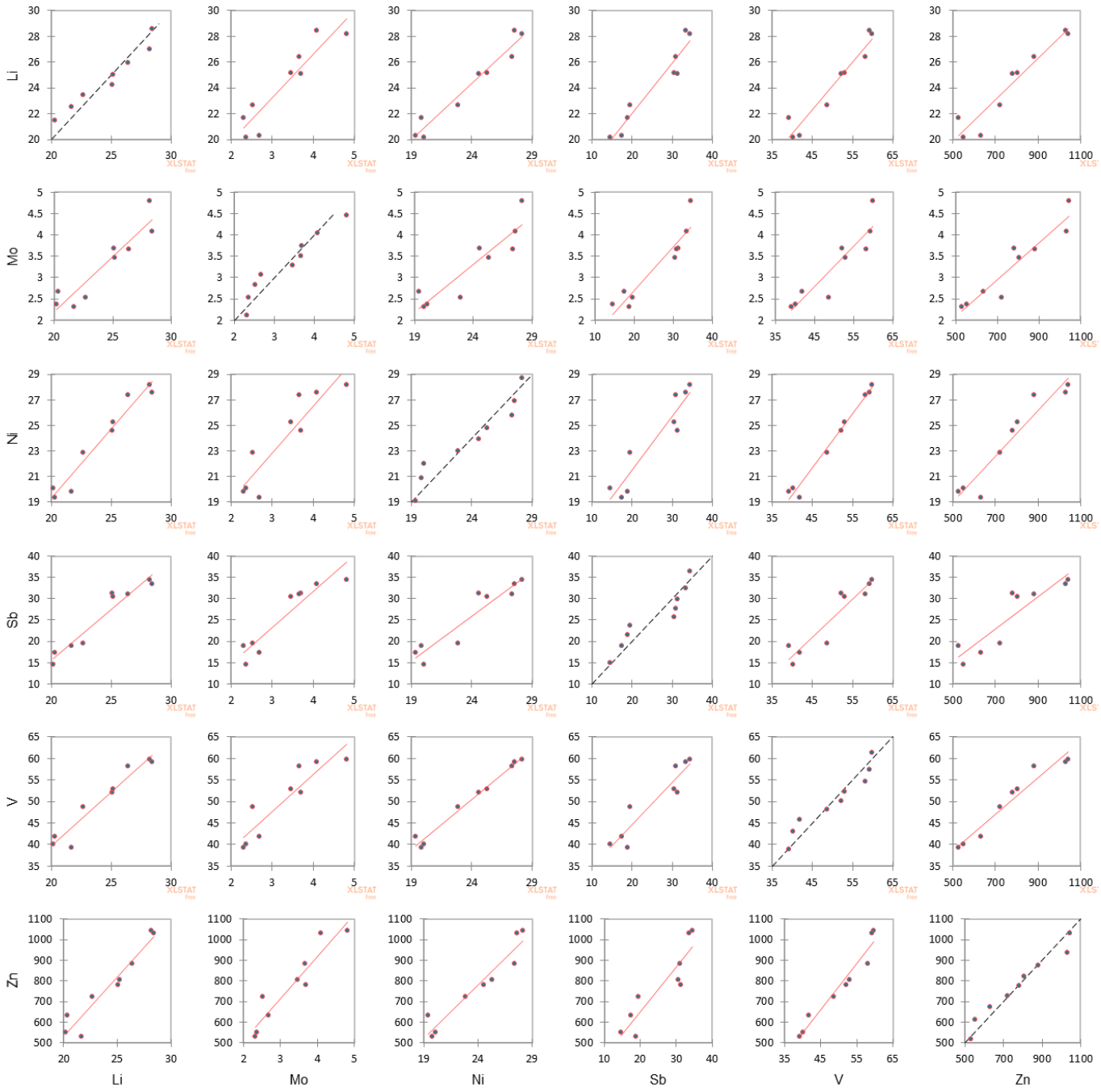

Figure SI 4d: Quantile-Quantile plots of SBR + BR, OM and metals variables using Microsoft Excel software and XLSTAT add-on.

Figure SI 5: SEM-EDX observation of a TRWP collected on a glassfiber filter using an instrumented vehicle from our previous study (De Oliveira *et al.* 2024). The observation demonstrates the presence of heteroaggregates in the emission plume, whose components consist of carbon (20-40%), terrigenous or ocean-derived minerals (Na, Si) and various metals (Sn, Zn, Fe, Mg).

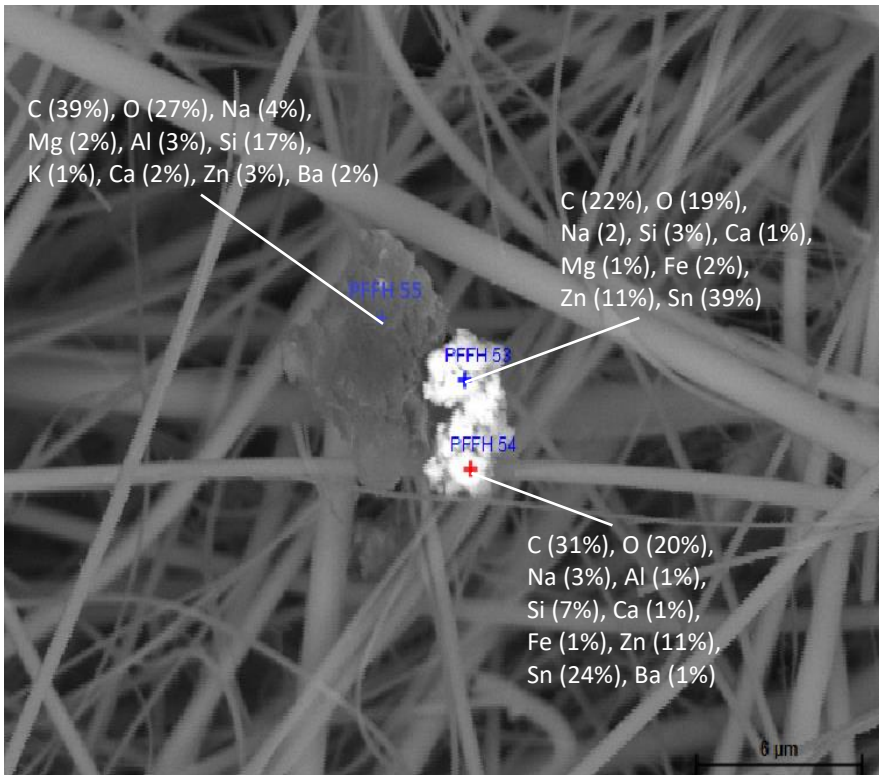

Figure SI 6: SEM-EDX observations of a heteroaggregate in the O_3 sediment sample suggest it is likely a TRWP, given its morphology similar to that of TRWP previously observed in Kreider *et al.*'s (2010) study. The aggregate also shows mineral and metal encrustations within an enriched carbonaceous matrix.

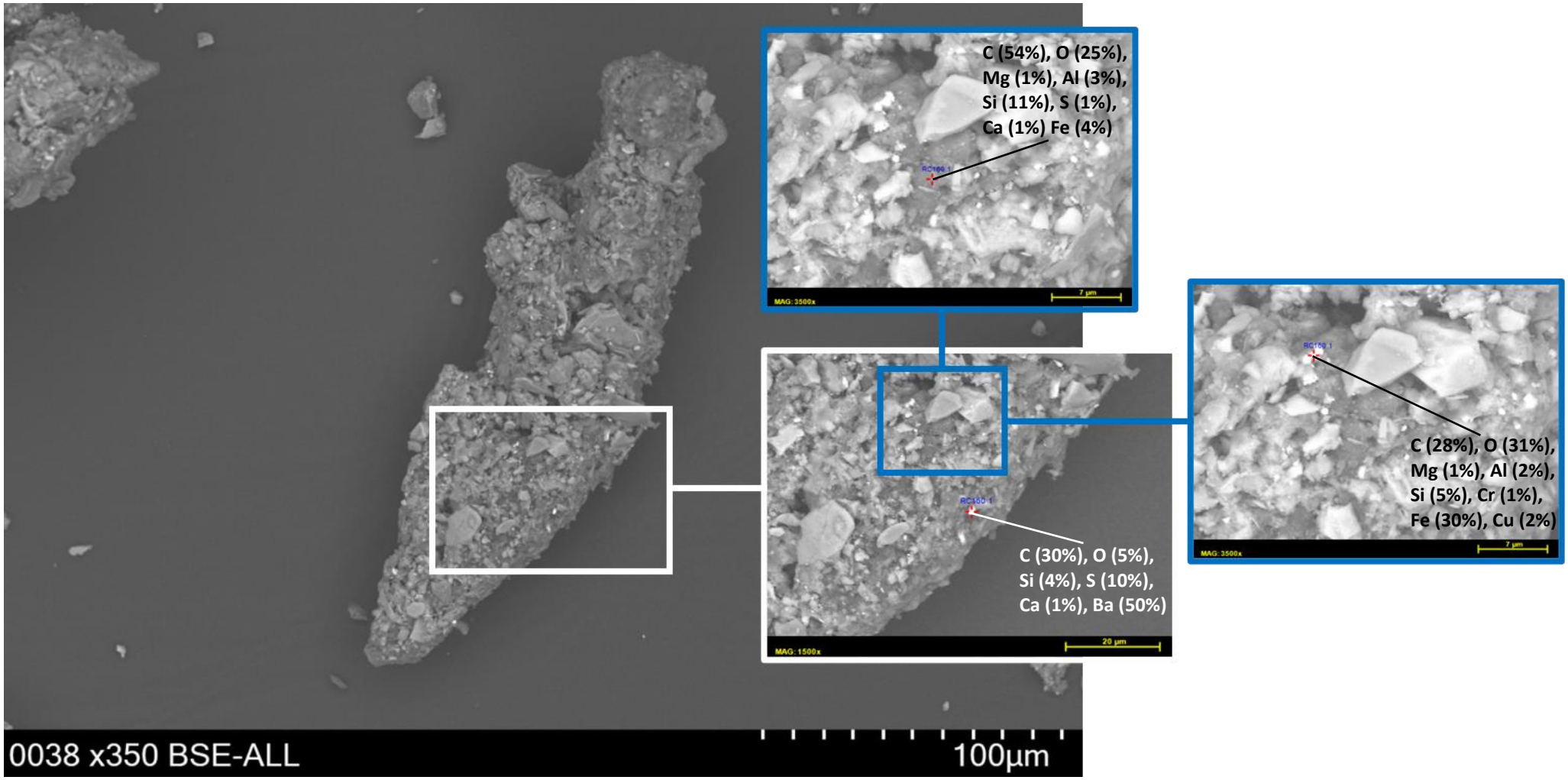

Table SI 1: Limit of quantification (LOQ) of the targeted metal elements in sediment matrix.

	As (mg/kg)	Cd (mg/kg)	Cr (mg/kg)	Cu (mg/kg)	Li (g/kg)	Mo (mg/kg)	Ni (mg/kg)	Sb (mg/kg)	V (mg/kg)	Zn (mg/kg)
LOQ	4	0.004	2	1	0.01	0.01	1	0.01	1	1

Table SI 2: Pyr-GC-MS setup and operating conditions.

Pyrolyzer	EGA/PY-3030D (FrontierLab)	
	Pyrolysis temperature (°C)	600
	Pyrolysis time (s^{-1})	12
Gas Chromatography	8890 (Agilent)	
	Injector temperature (°C)	300
	Carrier Gas	He
	Slip Ratio	46:1
	Pre-column	No
	Column	Ultra ALLOY^{+}-5 (30 m; 0.25 mm; 0.25 µm)
	Temperature program	50°C (hold 5min); 25°C.min^{-1}; 300°C (hold 10 min)
	Run Time (min)	25
Mass Spectrometer	5977B (Agilent) Single quad	
	Source temperature (°C)	230
	MS temperature (°C)	150
	Ionization energy (eV)	70
	Mass range (m/z)	50-400

Table SI 3: Theoretical TRWP amount retained in the sediment (kg) calculated from Equation 3 and considering three sediment density hypotheses: ρ_1, ρ_2 and ρ_3. These hypotheses correspond to silt, TRWP and coarser sediments with densities of 1.3, 1.8, and 2.6 g/cm^3, respectively.

Section of the infiltration pond	Sample	SBR+BR (mg/g)	TRWP (mg/g)	Surface area (m²)	Sediment thickness (m)	TRWP amount according to ρ_1 (kg)	TRWP amount according to ρ_2 (kg)	TRWP amount according to ρ_3 (kg)
Entrance	E_1	1.28 ± 0.05	11.64 ± 0.48	45	0.010	6.81 ± 0.28	9.42 ± 0.39	13.61 ± 0.56
	E_2	2.97 ± 0.07	27.11 ± 0.68	45		15.86 + 0.40	21.96 ± 0.55	31.72 ± 0.80
	E_3	2.06 ± 0.08	18.75 ± 0.77	45		10.97 + 0.45	15.19 ± 0.63	21.94 ± 0.90
	Sum					**33.64 ± 1.13**	**46.57 ± 1.57**	**67.27 ± 2.26**
Middle	M_1	2.99 ± 0.12	27.31 ± 1.12	86	0.015	45.98 ± 1.89	63.66 ± 2.62	91.96 ± 3.79
	M_2	5.54 ± 0.22	50.55 ± 1.99	86		85.10 ± 3.35	117.83 ± 4.64	170.20 ± 6.70
	M_3	4.99 ± 0.21	45.55 ± 1.88	86		76.69 ± 3.16	106.19 ± 4.37	153.38 ± 6.32
	Sum					**207.77 ± 8.40**	**287.68 ± 11.63**	**415.54 ± 16.81**
Overflow	O_1	1.80 ± 0.07	16.44 ± 0.68	72	0.020	30.77 ± 1.27	42.61 ± 1.75	61.55 ± 2.53
	O_2	7.05 ± 0.38	64.27 ± 3.48	72		120.31 ± 6.51	166.59 ± 9.01	240.63 ± 13.02
	O_3	7.15 ± 0.29	65.19 ± 2.68	72		122.03 ± 5.02	168.97 ± 6.96	244.07 ± 10.05
	Sum					**272.83 ± 12.80**	**378.17 ± 17.72**	**546.25 ± 25.60**
	$\boldsymbol{TRWP_{retained}}$					**514.24 ± 22.33**	**712.42 ± 30.92**	**1029.06 ± 44.67**

Table SI 4: Granulometric distribution of the sediment sieved at 2 mm.

Samples	d_{50} (µm)
E_1	114
E_2	95
E_3	104
M_1	99
M_2	83
M_3	59
O_1	101
O_2	70
O_3	59

Table SI 5: Enrichment factor calculated for the targeted metal elements in the sediment of the infiltration pond.

	As	Cd	Cr	Cu	Li	Mo	Ni	Sb	V	Zn
E_1	9.76	5.03	1.97	10.10	1.29	8.85	1.41	37.16	1.58	9.55
E_2	8.93	5.16	2.10	8.68	1.28	7.82	1.46	30.98	1.52	8.34
E_3	9.86	5.35	2.39	11.09	1.44	8.35	1.67	41.70	1.84	10.91
M_1	9.06	4.03	1.83	9.05	1.37	7.63	1.44	40.26	1.48	8.00
M_2	11.72	6.04	2.68	14.07	1.59	12.18	1.79	66.67	1.97	11.79
M_3	13.28	7.03	3.01	15.10	1.67	12.10	1.99	66.13	2.20	13.35
O_1	11.64	5.76	2.72	14.66	1.60	11.42	1.84	65.09	2.00	12.19
O_2	14.00	7.42	3.05	20.20	1.79	15.84	2.05	73.51	2.26	15.79
O_3	13.27	8.55	3.01	17.73	1.80	13.47	2.01	71.52	2.24	15.62

Table SI 6: Shapiro-Wilk parameter W and the associated p-value for SBR + BR, OM, and metals variables. The p-values are greater than 0.05, indicating a high probability that the data follow a normal distribution.

Variables	SBR + BR	OM	As	Cd	Cr	Cu	Li	Mo	Ni	Sb	V	Zn
W	0.8976	0.9453	0.8961	0.963	0.8968	0.9375	0.9162	0.917	0.8859	0.844	0.8885	0.937
p-value	0.2383	0.6384	0.2303	0.8289	0.2341	0.5556	0.3614	0.3678	0.1809	0.06392	0.1924	0.5504

Table SI 7: Spearman's rank correlation coefficient (above the grey diagonal) with associated p-values (below the grey diagonal). All p-values are below the 0.05 significance level for SBR + BR, OM, and metals variables. 'n.d.' stands for 'not determined' since the Spearman's coefficient is equal to one.

	SBR	OM	As	Cd	Cr	Cu	Li	Mo	Ni	Sb	V	Zn
SBR		0.945	0.805	0.918	0.839	0.740	0.839	0.720	0.904	0.873	0.775	0.775
OM	1.20E-04		0.901	0.988	0.925	0.864	0.956	0.771	0.984	0.925	0.874	0.874
As	8.83E-03	9.03E-04		0.942	0.937	0.949	0.975	0.928	0.936	0.963	0.919	0.919
Cd	4.71E-04	6.80E-07	1.49E-04		0.950	0.921	0.981	0.845	0.984	0.950	0.925	0.925
Cr	4.74E-03	3.57E-04	1.95E-04	8.63E-05		0.956	0.950	0.841	0.963	0.911	0.972	0.972
Cu	2.28E-02	2.69E-03	9.14E-05	4.13E-04	5.64E-05		0.949	0.924	0.918	0.925	0.986	0.986
Li	4.72E-03	5.57E-05	8.39E-06	2.99E-06	8.96E-05	9.49E-05		0.868	0.971	0.950	0.928	0.928
Mo	2.87E-02	1.50E-02	3.11E-04	4.12E-03	4.52E-03	3.75E-04	2.44E-03		0.811	0.939	0.892	0.892
Ni	8.17E-04	1.87E-06	2.09E-04	1.51E-06	2.96E-05	4.87E-04	1.32E-05	8.01E-03		0.939	0.926	0.926
Sb	2.14E-03	3.57E-04	3.12E-05	8.63E-05	6.44E-04	3.54E-04	8.96E-05	1.75E-04	1.78E-04		0.906	0.906
V	1.42E-02	2.09E-03	4.60E-04	3.46E-04	1.18E-05	9.54E-07	3.10E-04	1.23E-03	3.42E-04	7.59E-04		1.000
Zn	1.42E-02	2.09E-03	4.60E-04	3.46E-04	1.18E-05	9.54E-07	3.10E-04	1.23E-03	3.42E-04	7.59E-04	n.d	

References

De Oliveira, T., Muresan, B., Ricordel, S., Lumière, L., Truong, X.-T., Poirier, L., Gasperi, J., 2024. Realistic assessment of tire and road wear particle emissions and their influencing factors on different types of roads. J. Hazard. Mater. 465, 133301. https://doi.org/10.1016/j.jhazmat.2023.133301

Kreider, M.L., Panko, J.M., McAtee, B.L., Sweet, L.I., Finley, B.L., 2010. Physical and chemical characterization of tire-related particles: Comparison of particles generated using different methodologies. Sci. Total Environ. 408, 652–659. https://doi.org/10.1016/j.scitotenv.2009.10.016